Highly dispersed Pd nanoparticles on chemically modified graphene with aminophenyl groups for formic acid oxidation*

Yang Su-Dong(杨苏东)[a)b)], Shen Cheng-Min(申承民)[b)], Tong Hao(佟 浩)[a)], He Wei(何 卫)[a)], Zhang Xiao-Gang(张校刚)[a†], and Gao Hong-Jun(高鸿钧)[b)‡]

[a)] *College of Material Science and Engineering, Nanjing University of Aeronautics and Astronautics, Nanjing* 210016, *China*
[b)] *Beijing National Laboratory for Condensed Matter Physics, Institute of Physics, Chinese Academy of Sciences, Beijing* 100190, *China*

(Received 20 July 2011; revised manuscript received 18 August 2011)

A novel electrode material based on chemically modified graphene (CMG) with aminophenyl groups is covalently functionalized by a nucleophilic ring-opening reaction between the epoxy groups of graphene oxide and the aminophenyl groups of p-phenylenediamine. Palladium nanoparticles with an average diameter of 4.2 nm are deposited on the CMG by a liquid-phase borohydride reduction. The electrocatalytic activity and stability of the Pd/CMG composite towards formic acid oxidation are found to be higher than those of reduced graphene oxide and commercial carbon materials such as Vulcan XC-72 supported Pd electrocatalysts.

Keywords: chemically modified graphene, fuel cell, electrocatalysis, Pd nanoparticles

PACS: 33.20.Ea, 68.37.Lp, 81.10.Dn, 82.45.Jn **DOI:** 10.1088/1674-1056/20/11/113301

1. Introduction

Graphene, a new class of two-dimensional carbon nanostructure, has recently been of special interest to researchers actively engaged in nano-science because it possesses many fascinating properties such as giant electron mobility, extremely high thermal conductivity and extraordinary elasticity and stiffness.[1−7] Therefore, it has potential applications in many fields such as nanoelectronics, sensors, nanocomposites, batteries, supercapacitors and hydrogen storage.[8] In particular, graphene is a good heterogeneous catalyst-support material for direct liquid fuel cells, due to its high specific surface area, excellent electronic conductivity, and high chemical stability.[3,8,9] Much effort has been devoted to the synthesis of metal nanoparticles (NPs)-graphene hybrid composites.[10−12] However, graphene lacks sufficient binding sites for anchoring precursor metal ions or metal NPs, so it is important to find ways to deposit stable, well dispersed metal NPs on its surface. In order to disperse NPs homogeneously on the surface, it must be modified via suitable functionalization. One promising route to achieve mass production of chemically modified graphene (CMG) is to generate it from graphene oxide (GO). Researchers have suggested that GO contains plentiful, chemically reactive epoxy groups on its basal planes.[13,14] These epoxy groups can be easily modified through ring-opening reactions under various conditions. Wang et al.[15] demonstrated an epoxide ring-opening reaction by means of adding octadecylamine to a dispersion of GO, producing colloidal suspensions of CMG platelets in organic solvents. In a relevant study, an ionic liquid with an amine end group was attached to GO platelets via the ring-opening reaction with epoxy groups.[16] This strategy could increase the number of surface nucleation sites for NPs.

In this study, we report on the fabrication of CMG with aminophenyl groups as a catalyst-support by means of a nucleophilic ring-opening reaction between the epoxy groups of GO and the aminophenyl groups of p-phenylenediamine (PPD). After this reaction,

*Project supported by the National Basic Research Program of China (Grant No. 2007CB209700), the Graduate Student Innovation Foundation of Jiangsu Province, China (Grant No. CX09B_075Z), and the Research Funding of Nanjing University of Aeronautics and Astronautics, China (Grant No. NS2010165).

†Corresponding author. E-mail: azhangxg@163.com
‡Corresponding author. E-mail: hjgao@aphy.iphy.ac.cn

© 2011 Chinese Physical Society and IOP Publishing Ltd

palladium NPs are directly reduced onto the CMG supports. Our results show that Pd/CMG exhibits excellent catalytic activity and stability for formic acid oxidation in comparison with reduced graphene oxide (RGO) and Vulcan XC-72 supported Pd electrocatalysts .

2. Experiment

2.1. Materials

The graphite powder (SP grade), palladium chloride ($PdCl_2$), hydrazine hydrate, sodium borohydride ($NaBH_4$) and PPD were purchased from Sinopharm Chemical Reagent Co. Ltd., China. Potassium hydroxide (KOH) was obtained from Nanjing Chemicals, China. Unless otherwise stated, other reagents were of analytical grade and were used as received.

2.2. Synthesis of CMG and Pd/CMG composites

The GO was prepared according to a modified Hummer's method.[17] CMG with aminophenyl groups was synthesized between GO and PPD. 100 mg of PPD was added into 100 mL of a homogeneous, transparent GO (0.5 mg·mL^{-1}) dispersion in water. Then, 100 mg of KOH was added into the mixture and the mixture was subjected to ultrasonication for 30 min. Finally, the homogeneous solution was vigorously stirred at 80 °C for 24 h. After centrifuging and rinsing with water and ethanol several times, the resulting product was redispersed in 100 mg water. Then, 1 mL hydrazine hydrate was added into the dispersion and the reaction mixture was kept at 100 °C for 24 h under constant stirring.[18] The final products were centrifuged, washed and finally air-dried. For comparison, RGO was prepared by reduction of GO with hydrazine hydrate as described above.

Pd/CMG composite was synthesized by using $NaBH_4$ as a reductive agent at room temperature. 20 mg CMG was dissolved in water by ultrasonic treatment for 2 h and 0.72 mL of 7 mg·mL^{-1} $PdCl_2$ solution was added under stirring. The pH value of this mixture was adjusted to 6.5 using 1 M NaOH. Then, 100 mg of $NaBH_4$ was slowly added into the mixture with stirring for 12 h at room temperature. The resulting slurry was centrifuged, washed with deionized water and then dried in a vacuum oven. For comparative purposes, the same procedure was followed for the syntheses of Pd/RGO and Pd/Vulcan XC-72(C).

2.3. Preparation of electrode

Glassy carbon (GC) electrodes, 5 mm in diameter (electrode area 0.2 cm^2), polished with 0.05 μm alumina to a mirror-finish before each experiment, were used as substrates for supported catalysts. For the electrode preparation, typically, 3 mg of catalyst was added into 0.5 mL 0.05 wt.% Nafion solution and then the mixture was ultrasonicated for 1 h for uniform dispersion. A measured volume (30 μL) of this mixture was dropped by a microsyringe onto the top surface of the GC electrode. The as-obtained catalyst-modified GC electrode was employed as the working electrode in our experiments.

2.4. Characterization

Infrared spectra were recorded with a model 360 Nicolet AVATAR Fourier transform infrared (FT–IR) spectrophotometer. X-ray photoelectron spectroscopy (XPS) was recorded on an ASTM E1829-02 system. The analysis of the composition of the catalyst was obtained with a Thermo IRIS Intrepid II inductively coupled plasma atom emission spectrometry (ICP-AES) system. X-ray diffraction (XRD) analysis was performed on Bruker D8-ADVANCE diffractometer with Cu Ka radiation at a wavelength of $\lambda = 0.15418$ nm. Transmission electron microscopy (TEM, JEOL JEM-2100) was used to investigate the morphology of samples.

2.5. Electrochemical measurement

All electrochemical measurements were carried out with CHI 660c electrochemical workstation, using a three-electrode test cell. A conventional three-electrode system was used with a modified GC electrode as the working electrode (5 mm in diameter), a Pt wire as the counter electrode and a saturated calomel electrode (SCE) as the reference electrode. All electrolytes were deaerated by bubbling N_2 for 20 min and protected with a nitrogen atmosphere during the entire experimental procedure. All experiments were carried out at a temperature of (25 ± 1) °C.

3. Results and discussion

We used FT–IR analysis of CMG to confirm covalent interactions for the nucleophilic ring-opening reaction between GO and PPD. Before recording the FT–IR spectra, the CMG was washed with water and

ethanol repeatedly in order to get rid of any impurities.

Figure 1 shows the FT–IR spectra of CMG and PPD. By comparison with the infrared spectra, we see that the CMG exhibits peaks corresponding to the C=C stretching of quinonoid (1575 cm^{-1}) and benzenoid rings (1508 cm^{-1}), C–N stretching of the aromatic amine (1220 cm^{-1}), aromatic C–H in-plane bending (1160 cm^{-1}) and out-of-plane deformation of C–H in a 1,4-disubstituted benzene ring (829 cm^{-1}).[19] Moreover, the peaks at 3200 and 3310 cm^{-1} can be assigned to the $-NH_2$ of aminophenyl groups. It is worth noting that some bands of PPD are shifted toward lower wavenumbers in the CMG composition. The spectral red-shift phenomena of chemically synthesized nanocomposite result from the interaction between the CMG and PPD in accordance with a recent report.[20] The spectral red-shift phenomena of chemically synthesized nanocomposite result from the aminophenyl groups grafted on the CMG nanosheets basal plane. Such a shift could be an evidence for the CMG with aminophenyl group formation between PPD and GO caused by nucleophilic ring-opening reaction between the epoxy groups of GO and the aminophenyl groups of PPD. Thus, it is clear that the aminophenyl groups were well attached to the CMG surface.

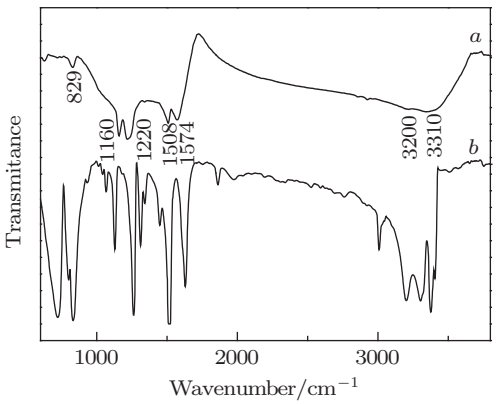


Fig. 1. FT–IR spectra of CMG (curve *a*) and PPD (curve *b*), indicating that aminophenyl groups have been successfully modified on the surface of CMG.

To further illustrate the covalent functionalization, the XPS of CMG samples is given in Fig. 2. As shown in Fig. 2(a), the XPS survey scan spectrum exhibits distinct C 1s, N 1s and O 1s peaks. As exhibited in the inset of Fig. 2(a), the N 1s spectrum shows a single component peak at 399.5 eV, which indicates that the experimental procedure was effective for grafting aminophenyl groups onto the CMG.[21,22] Consequently, the aminophenyl groups are grafted to the surface of the CMG. A shoulder of the main NH_2 peak is observed at 401.5 eV and is associated with the presence of the ammonium species. The C1s XPS spectrum of CMG (Fig. 2(b)) exhibits an additional component at 285.7 eV, and the new component can be assigned to the combination of the C bound to nitrogen, which appeared after the ring-opening reaction and the C–N groups forming from the aminophenyl groups of PPD. These results, combined with the FT–IR spectra, prove that the covalent reaction between the aminophenyl groups of PPD and the epoxy groups on the GO sheets occurred successfully.

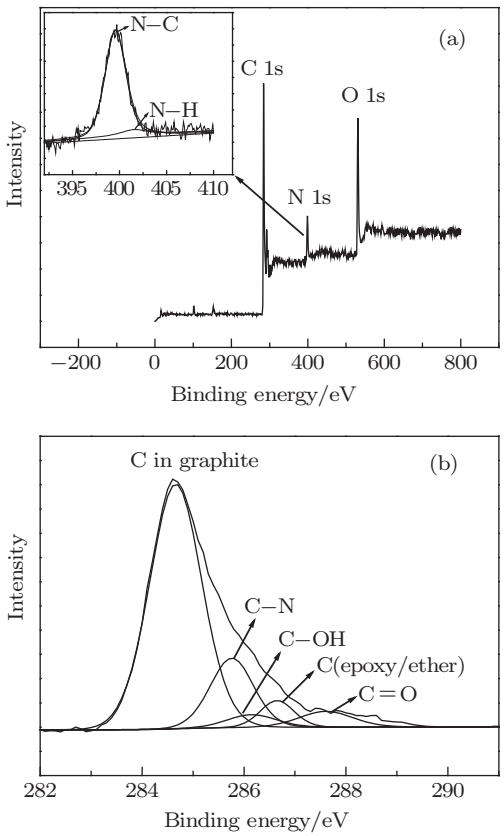


Fig. 2. XPS spectra of CMG: (a) XPS full spectrum of CMG, (b) higher resolution data of the C1s of CMG, indicating that CMG surface have been modified with aminophenyl groups.

In order to compare the influence of different supporting materials on morphology of Pd NPs, we use TEM technique to analyse the shape and size distributions of the Pd NPs loaded on the three supporting materials. The three supporting materials are modified graphene sheets, reduced graphene oxide sheets and Vulcan XC-72 carbon powder, separately. The preparation of Pd NPs loaded on supporting materials is under the same condition. The TEM images and patterns of Pd NPs size distribution are shown in Fig. 3. From Fig. 3(a), it is seen clearly that Pd NPs

are uniformly distributed on the chemically modified graphene sheets. This observation contrasts with the results of control experiments in which the Pd NPs are deposited on RGO (Fig. 3(c)) surfaces where particles of various sizes exist mostly as aggregates and are distributed randomly. In Fig. 3(e), Pd NPs deposited on Vulcan XC-72 (Pd/C) also show a large size distribution of Pd particles that aggregated significantly in many regions. Results show that the mean sizes of Pd NPs are (4.2 ± 0.8) nm, (4.6 ± 1.1) nm and (5.5 ± 1.3) nm for Pd/CMG, Pd/u-CMG and Pd/C, respectively. The small diameter and relatively narrow diameter distribution of Pd NPs on CMG is due to the immobilization of bifunctional aminophenyl groups, which offers uniformly distributed active sites for anchoring metal ions. In addition, the aminophenyl groups on CMG can effectively avert the aggregation of CMG and thus lead to water-dispersible graphene sheets. This composite provides highly effective surface areas of CMG for subsequent deposition of Pd NPs. Highly dispersed metal NPs on supports with larger surface areas have advantages in catalytic activity and sensor sensitivity. This unique structure appears to provide a suitable support for many uniform Pd NPs, thereby favouring high performance in formic acid oxidation, as discussed below.

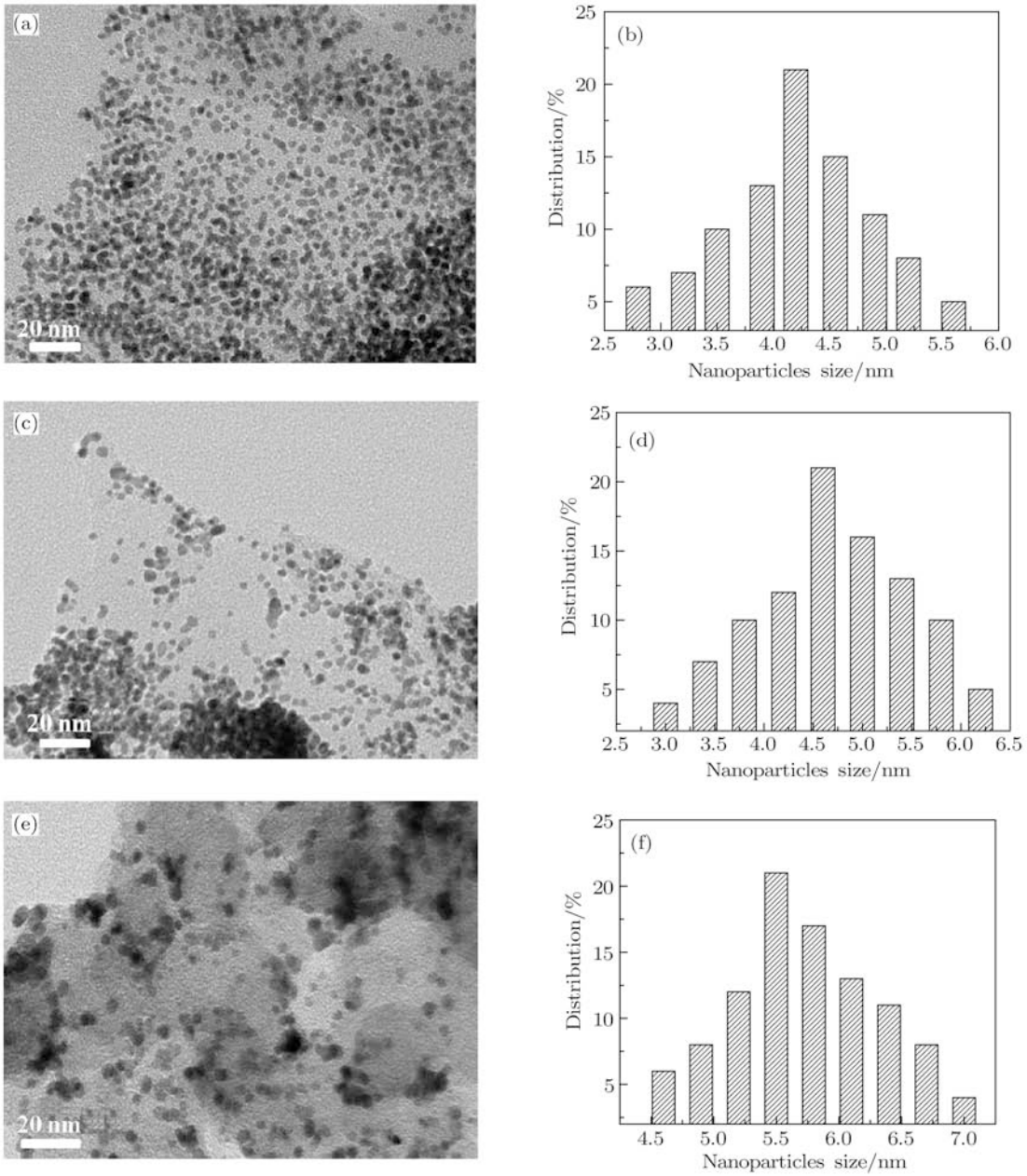


Fig. 3. TEM images and particle size distribution histograms of Pd/CMG ((a) and (b)), Pd/RGO ((c) and (d)), and Pd/C ((e) and (f)), indicating Pd NPs have been deposited on the surface of CMG.

Here, we propose a possible formation mechanism for Pd catalyst NPs on CMG. When the pH of the solution is controlled at slight acidity, the aminophenyl groups on the CMG surface become weakly positive charge.[23] It leads to the electrostatic interaction between the negative $PdCl_4^{2-}$ ions and positively charged functional groups of aminophenyl on the CMG, forming a uniformly distributed Pd ion precursors on the surface of CMG. Finally, sodium borohydride is added into this mixed solution to reduce the Pd precursors. The electrostatic interaction between Pd ions and GMG resulted in uniform and dispersive formation of Pd NPs on the CMG surface. On the other hand, this strategy could increase the number of surface nucleation sites for NPs.

The XRD patterns of the different composites are shown in Fig. 4. The GO pattern (pattern *a* in Fig. 4) has a strong diffraction peak at a 2θ value of 9.7° with a corresponding d-spacing of 0.91 nm. The increased interlayer spacing for GO can weaken the van der Waals interaction between layers and make exfoliation via sonication easier.[24] However, it is worth noting that no obvious peaks attributable to GO could be found for the CMG samples (pattern *b* in Fig. 4), confirming the reduction of the GO sheets and indicating that CMG was obtained successfully in this work. In conclusion, well-exfoliated GO and CMG were successfully obtained in this work. The XRD patterns of various Pd-carbon nanocomposites are shown in patterns $c-e$ of Fig. 4. Characteristic diffraction peaks of Pd(111) at 39.6° and Pd(200) at 45.5° for a face-centered cubic (fcc) structure were also observed. Pattern *e* in Fig. 4 shows that the Pd (111) band at 39.6° is very broad for the CMG nanomaterial, which is in contrast to the sharp and narrow bands for Pd NPs on RGO nanomaterials (pattern *d* in Fig. 4). The figure indicates the smaller size of Pd NPs on the CMG sheets. The application of Scherrer's[25] equation to the broadening of the Pd(111) peak shows that the average sizes of the Pd NPs for Pd/CMG, Pd/RGO, and Pd/C are 4.2, 4.6, and 5.5 nm, respectively.

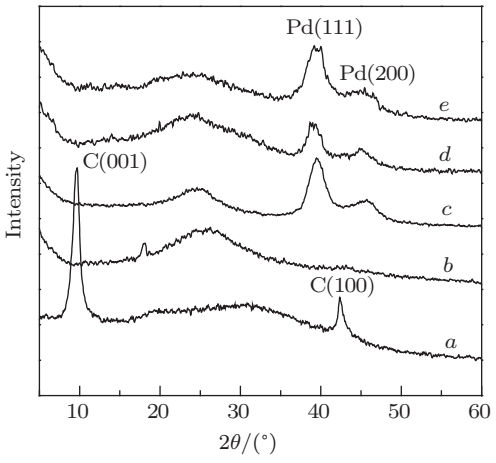


Fig. 4. XRD patterns of GO (curve *a*), CMG (curve *b*), Pd/C (curve *c*), Pd/RGO (curve *d*) and Pd/CMG (curve *e*).

The practical compositions of Pd in different samples were evaluated by ICP-AES analysis. The Pd/CMG, Pd/RGO and Pd/C catalysts had the metal loadings of 30.1, 28.2, and 27.6 wt%, respectively. The oxidation currents of cyclic voltammograms and chronoamperometry tests were normalized to the measured metal loading for further comparing the activities of different catalysts. The electrochemically active surface area (ECSA) provides important information regarding the number of available active sites.[26] Figure 5 shows cyclic voltammograms of different electrocatalysts that are in contact with 0.25 M H_2SO_4. All potentials were referred to the saturated calomel electrode (SCE) in this work. Typical hydrogen and oxygen adsorption/desorption behaviours on Pd can be clearly observed on the samples. The ECSA was estimated by integrating the voltammogram corresponding to hydrogen desorption (Q_H) by adapting the assumption of 212 $\mu C \cdot cm^{-2}$ from the electrode surface. The ECSA for Pd/C, Pd/RGO and Pd/CMG were estimated to be 107.5, 123.2, and 155.6 $m^2 \cdot g^{-1}$, respectively. This indicates that the Pd/CMG catalyst has a larger ECSA, which can be attributed to the uniform distribution and small particle size of Pd NPs on CMG. This result demonstrates that Pd NPs deposited on CMG are electrochemically more accessible, which is very important for electrocatalytic applications in fuel cells. In addition, the double layer capacitance was also obtained from

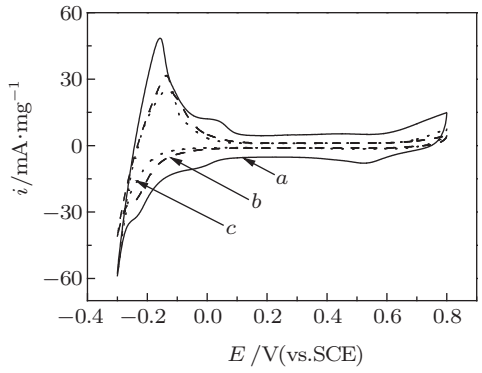


Fig. 5. Cyclic voltammograms of different composites in 0.25 M H_2SO_4 solution at a scan rate of 20 $mV \cdot s^{-1}$ for Pd/CMG (curve *a*), Pd/RGO (curve *b*) and Pd/C (curve *c*).

the cyclic voltammetry data. The electrical capacitance is a measure of the surface area. The increased double-layer thickness of the Pd/CMG based electrodes reflects the higher specific surface area of the support composite.

The high ECSA for the Pd/CMG material is also supported by the high electrocatalytic activity for electro-oxidation of formic acid. The obtained cyclic voltammetry (CV) curves exhibit very prominent characteristic peaks for formic acid oxidation. Figure 6 compares the formic acid oxidation activities of the three Pd catalysts in 0.25 M H_2SO_4 containing 0.25 M HCOOH. As shown in Fig. 6, the highest HCOOH oxidation current density can be observed in the Pd/CMG sample, indicating the highest catalytic activity for HCOOH oxidation. The current densities of Pd/CMG, Pd/RGO and Pd/C, calculated from the forward-scan, were 112.36, 70.13, 52.25 $mA\cdot mg^{-1}$ at 0.11 V, respectively. The higher electrocatalytic activity for the formic acid oxidation on Pd/CMG than those on Pd/RGO and Pd/C shows the importance of the distribution and the dispersion of Pd electrocatalysts on CMG supports. This is an important improvement for the Pd catalyst because the use of CMG as the support material can significantly reduce the amount of unit loading to achieve the same performance as that of the Pd/CMG.

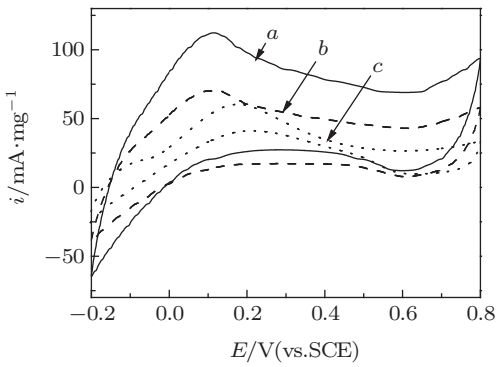


Fig. 6. Cyclic voltammograms of different composites in 0.25 M H_2SO_4 + 0.25 M HCOOH solution at a scan rate of 50 $mV\cdot s^{-1}$ for Pd/CMG (curve *a*), Pd/RGO (curve *b*) and Pd/C (curve *c*).

The chronoamperometric technique is an effective method to evaluate the electrocatalytic stability of catalyst materials. Figure 7 shows the typical current density-time responses of Pd-based catalysts for formic acid electro-oxidation. The polarization currents for the formic acid oxidation reaction on the three catalysts each shows a significant decay initially and reach a stable value after being polarized at 0.1 V for 600 s. The current decay for the HCOOH oxidation reaction indicates the slow deactivation of Pd-based electrocatalysts by the adsorption of CO or CO-like intermediates.[27,28] However, in the steady-state region, Pd/CMG composites present a current density of 20.68 $mA\cdot mg^{-1}$, while Pd/RGO and Pd/C composites exhibit current densities of about 9.99 and 2.15 $mA\cdot mg^{-1}$, respectively. This indicates that Pd/CMG catalyst also has a much higher stability toward the poisoning by adsorbed CO or CO-like intermediate species during the HCOOH oxidation as compared with Pd/RGO and Pd/C catalysts. The significant enhancement in the catalytic activity and stability of Pd/CMG catalyst as compared with Pd/RGO and Pd/C catalysts may be attributed to the better uniformly distributed and smaller Pd NPs supported on CMG.

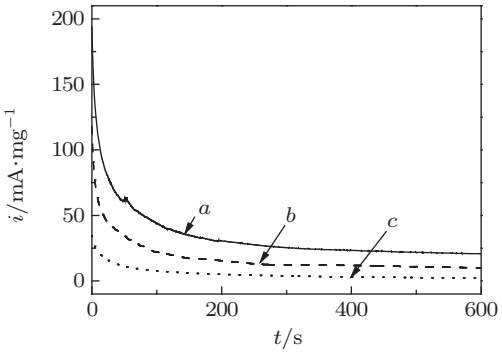


Fig. 7. Chronoamperometric curves for different composites in 0.25 M H_2SO_4 + 0.25M HCOOH solution of 0.1 V for Pd/CMG (curve *a*), Pd/RGO (curve *b*) and Pd/C (curve *c*).

These favourable properties may result from three factors. First, CMG with aminophenyl groups can greatly enhance the nucleation of nanocrystalline metals onto CMG by providing a large number of hydrophilic molecular groups on the surface.[29] These heterogeneous nucleation sites facilitate the deposition of finer, better dispersed Pd NPs, a highly desirable feature for Pd catalyst applications. Additionally, the specific interactions between the aminophenyl groups on the CMG and $PdCl_4^{2-}$ could lead to the deposition of Pd NPs in a narrower size distribution.[30] Well-dispersed Pd NPs on the Pd/CMG hybrid structure likely give rise to more phase boundaries, which in turn improves the catalytic efficiency. Finally, the CMG sheets each have a large surface area and the particles can be deposited on both sides of these sheets. On the other hand, the large surface areas may facilitate the transmission of the electrolyte and formic acid through the surface of the catalyst.

4. Conclusion

The CMG with aminophenyl groups is successfully synthesized as catalyst-supports by a nucleophilic ring-opening reaction between GO and PPD. The CMG sheets are used as support materials for Pd NPs and the electrochemical properties of assemblies for formic acid oxidation are investigated. The superior performance of Pd/CMG is attributed to the better uniform distribution and dispersion with narrow particle size distribution. It is envisaged that both the ease and the convenience of the strategy developed in this study make it an attractive alternative for large-scale and cost-effective production of CMG, as well as for the deposition of a variety of metal NPs on CMG for other heterogeneous catalyst applications.

References

[1] Kim K S, Zhao Y, Jang H, Lee S Y, Kim J M, Kim K S, Ahn J H, Kim P, Choi J Y and Hong B H 2009 *Nature* **457** 706

[2] Schedin F, Geim A K, Morozov S V, Hill E W, Blake P, Katsnelson M I and Novoselov K S 2007 *Nature Mater.* **6** 652

[3] Stankovich S, Dikin D A, Dommett G H B, Kohlhaas K M, Zimney E J, Stach E A, Piner R, Nguyen S T and Ruoff R S 2006 *Nature* **442** 282

[4] Stoller M D, Park S J, Zhu Y W, An J H and Ruoff R S 2008 *Nano Lett.* **8** 3498

[5] Novoselov K S, Geim A K, Morozov S V, Jiang D, Zhang Y, Dubonos S V, Grigorieva I V and Firsov A A 2004 *Science* **306** 666

[6] Gao M, Pan Y, Zhang C D, Hu H, Yang R, Lu H L, Cai J M, Du S X, Liu F and Gao H J 2010 *Appl. Phys. Lett.* **96** 053109

[7] Pan Y, Zhang H G, Shi D X, Sun J T, Du S X, Liu F and Gao H J 2009 *Adv. Mater.* **21** 2777

[8] Geim A K and Novoselov K S 2007 *Nature Mater.* **6** 183

[9] Behabtu N, Lomeda J R, Green M J, Higginbotham A L, Sinitskii A, Kosynkin D V, Tsentalovich D, Parra-Vasquez A N G, Schmidt J, Kesselman E, Cohen Y, Talmon Y, Tour J M and Pasquali M 2010 *Nature Nanotechnol.* **5** 406

[10] Li Y M, Tang L H and Li J H 2009 *Electrochem. Commun.* **11** 846

[11] Li Y J, Gao W, Ci L J, Wang C M and Ajayan P M 2010 *Carbon* **48** 1124

[12] Shang N G, Papakonstantinou P, Wang P, Silva S and Ravi P 2010 *J. Phys. Chem.* C **114** 15837

[13] He H Y, Klinowski J, Forster M and Lerf A 1998 *Chem. Phys. Lett.* **28 7**53

[14] Lerf A, He H Y, Forster M and Klinowski J 1998 *J. Phys. Chem.* B **102** 4477

[15] Wang S, Chia P J, Chua L L, Zhao L H, Png R Q, Sivaramakrishnan S, Zhou M, Goh R G S, Friend R H, Wee A T S and Ho P K H 2008 *Adv. Mater.* **20** 3440

[16] Yang H F, Shan C S, Li F H, Han D X, Zhang Q X and Niu L 2009 *Chem. Commun.* **26** 3880

[17] Hummers W S and Offeman R E 1958 *J. Am. Chem. Soc.* **80** 1339

[18] Stankovich S, Dikin D A, Piner R D, Kohlhaas K A, Kleinhammes A, Jia Y, Wu Y, Nguyen S T and Ruoff R S 2007 *Carbon* **45** 1558

[19] Ellison M D and Gasda P J 2008 *J. Phys. Chem.* C **112** 738

[20] Wang H L, Hao Q L, Yang X J, Lu L D and Wang X 2009 *Electrochem. Commun.* **11** 1158

[21] Roodenko K, Gensch M, Rappich J, Hinrichs K, Esser N and Hunger R 2007 *J. Phys. Chem.* B **111** 7541

[22] Martin C, Alias M, Christien F, Crosnier O, Belanger D and Brousse T 2009 *Adv. Mater.* **21** 4735

[23] Wang S Y, Wang X and Jiang S P 2008 *Langmuir* **24** 10505

[24] Hontoria-Lucas C, López-Peinado A J, López-Gonzáez J de D, Rojas-Cervantes M L and Martín-Aranda R M 1995 *Carbon* **33** 1585

[25] Ding H, Shi X Z, Shen C M, Hui C, Xu Z C, Li C, Tian Y, Wang D K and Gao H J 2010 *Chin. Phys.* B **19** 106104

[26] Seger B and Kamat P V 2009 *J. Phys. Chem.* C **113** 7990

[27] Yu X W and Pickup P G 2009 *Electrochem. Commun.* **11** 2012

[28] Miyake H, Okada T, Samjeske G and Osawa M F 2008 *Phys. Chem. Chem. Phys.* **10** 3662

[29] Guo D J and Li H L 2005 *Carbon* **43** 1259

[30] Guo Z P, Han D M, Wexler D, Zeng R and Liu H K 2008 *Electrochim. Acta* **53** 6410